

ASTROMETRIC IMAGING OF CROWDED STELLAR FIELDS WITH ONLY TWO SIM POINTINGS

NEAL DALAL & KIM GRIEST

Physics Dept., University of California, San Diego, CA 92093

endall@astrophys.ucsd.edu, griest@astrophys.ucsd.edu

Draft version November 10, 2018

ABSTRACT

The Space Interferometry Mission (SIM) will observe sources in crowded fields. Recent work has shown that source crowding can induce significant positional errors in SIM's astrometric measurements, even for targets many magnitudes brighter than all other crowding sources. Here we investigate whether the spectral decomposition of the fringe pattern may be used to disentangle the overlapping fringes from multiple blended sources, effectively by performing synthesis imaging with two baselines. We find that spectrally dispersed fringes enable SIM to identify and localize a limited number of field sources quite robustly, thereby removing their effect from SIM astrometry and reducing astrometry errors to near photon noise levels. We simulate SIM measurements of the LMC, and show that (a) SIM astrometry will not be corrupted by blending and (b) extremely precise imaging of mildly crowded fields may be performed using only two orthogonal baseline orientations, allowing microarcsecond positional measurements. We lastly illustrate the method's potential with the example of astrometric microlensing, showing that SIM's mass and distance measurements of lenses will be untainted by crowding.

1. INTRODUCTION

The Space Interferometry Mission (SIM) will perform astrometry with unprecedented precision, measuring positions at the microarcsecond level. This will allow numerous astrophysical experiments to be performed that previously were impossible. Even though its 10 meter baseline allows resolution only of ~ 10 mas, SIM achieves microarcsecond astrometric precision by centroiding fringes to better than 1 part in a thousand. If SIM can meet its technical specifications, the primary source of error for single star astrometry would be photon noise, which can be beat down as $1/\sqrt{N}$ until the systematic error floor is reached. For multiple stars in the field of view, however, other errors may be incurred. For example, the extra flux of photons from field sources gives additional photon noise, which increases the amount of on-source integration time to achieve a given astrometric precision. Another source of error, which cannot be reduced by further integration time, is the distortion in the measured fringe pattern caused by the superposition of fringes from multiple incoherent sources. Since SIM achieves its revolutionary precision by fitting the observed fringe pattern in exquisite detail, even small scale deviations from the single star fringe pattern can lead to large astrometric errors. Several possible SIM experiments, such as microlensing, globular cluster dynamics, or stellar motions in external galaxies like M31, require SIM astrometry in crowded fields, and so it is necessary to determine whether or not crowding will corrupt SIM measurements irretrievably.

One might imagine that SIM astrometry of targets many magnitudes brighter than other sources in the field of view would be unaffected by the presence of those sources. However, Rajagopal et al. (2001) have recently shown that source confusion in crowded fields can lead to significant errors (\sim few μ as) in individual position measurements, even when the confusing field sources are just a few percent of the target's brightness. Such errors are comparable

to those expected from photon noise and systematic error, and could pose a serious threat to astrometric measurements in crowded fields if uncorrected. Brighter sources, such as binary companions or highly luminous field stars $\gtrsim 5\%$ in brightness, could completely destroy SIM astrometry. To correct these measurements, one would like to know the positions and brightnesses of all the important sources in the field of view – that is, one would like an image. A possibility is to obtain, prior to SIM observations, either space telescope or ground based adaptive optics (AO) snapshots of the field. Unfortunately, as we show below, the rough positions obtainable (~ 40 mas) from such images are of insufficient precision to rectify SIM astrometry. Another alternative is to perform synthesis imaging with SIM. In analogy to radio interferometry, one might orient SIM along numerous baselines, using multiple siderostat pairs to fill in the (u, v) plane (Allen 2000). Note, however, that a possible SIM design currently under consideration involves just one 10 meter baseline. A third alternative, which we discuss here, is to use SIM in its astrometry mode. If the sources all lie several fringes away from each other then the (u, v) coverage obtained from just two baselines, using multiple frequency channels, is sufficient to disentangle the sources from each other and measure all of their positions to few μ as precision. This is a marked increase in astrometric precision relative to that possible from SIM imaging, ~ 250 μ as (Allen 2000), and thus allows significantly improved proper motion measurements. We show that, for the currently expected characteristics of the SIM satellite, and for typical levels of crowding in the LMC, Bulge, and the outer regions of globular clusters, these two orthogonal baselines are adequate to achieve excellent astrometric or proper motion precision. Note that similar ideas have been used previously in simulations of closure phase measurements (Schloerb 1990) and in visibility measurements of the binary star Capella (Koechlin et al. 1979).

To see why just two baselines are sufficient, consider a synthesis imaging measurement of several point sources. This involves measuring the complex visibility \mathcal{V} at numerous points in the (u, v) plane, where $u = B_x/\lambda$, $v = B_y/\lambda$ are spatial frequencies, and B_x and B_y are the projections of the baseline separation along the x, y axes respectively. The visibility $\mathcal{V}(u, v)$ and brightness distribution $F(x, y)$ are related by Fourier transformation, e.g. $\mathcal{V}(u, v) = \int dx dy F(x, y) \exp(-2\pi i[ux + vy])$, via the van Cittert-Zernike theorem (see for example Lawson 2000, Chapter 2). For an arbitrary brightness distribution $F(x, y)$ sufficiently many u, v points must be sampled to permit accurate Fourier inversion of the visibility. A typical astrometry measurement relies upon just two baseline orientations, which would appear insufficient to localize more than one source position (x and y coordinates). Note, however, that each frequency channel at a given baseline orientation constitutes an independent u, v measurement, since $u = kB_x/2\pi$, $v = kB_y/2\pi$ (Schloerb 1990). The multifrequency u, v coverage from two orthogonal SIM baselines is limited to points on the u, v axes (see Figure 1), and is clearly insufficient to reconstruct an arbitrary brightness distribution. For *point sources*, on the other hand, this coverage suffices. Consider $F(x, y) = \sum_i F_i(k) \delta(x - x_i) \delta(y - y_i)$ corresponding to a sum of point sources, each with spectrum $F_i(k)$. Taking for now each F_i independent of k gives the measured visibility as $\mathcal{V}(u, v) = \sum_i F_i \exp(-2\pi i[x_i u + y_i v])$. Now, instead of the usual 2D Fourier transform to recover the brightness distribution, consider a single 1D Fourier transform, say along the u direction. This gives $\sum_i f_i(v) \delta(x - x_i)$, and similarly for the 1D transform along the v direction. Clearly, the sources' x coordinates are measurable just by sampling the visibility at multiple u along a line of constant v , and similarly for the y positions. By placing each source on a color-magnitude diagram (CMD) using the $F_i(k)$, the x sources can be matched up with the y sources, giving the unique 2D coordinates of each bright source in the field (Dyck et al. 1995). If the pairing is not obvious from the CMD, then a third baseline orientation is required to match up the x and y sources, but note that this need be done only once, at any time. In theory, therefore, the two orthogonal SIM baselines required to perform single source astrometry are all that are necessary to perform imaging of point sources. In practice, finite bandwidth, Nyquist sampling and photon noise will limit point source resolution. We explore these effects in the next section.

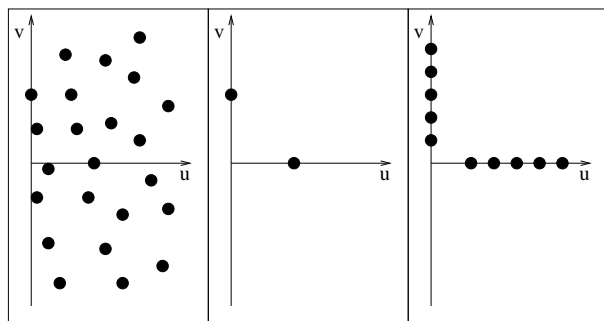


FIG. 1.— Schematic depictions of (u, v) coverage for (a) synthesis imaging with many baseline orientations, (b) astrometry with two baseline orientations, and (c) astrometry with two baselines and channeled spectrum. Only half of the (u, v) plane is illustrated since the brightness distribution is real; redundant points are not plotted.

2. FITTING DISPERSED FRINGES

The above procedure of Fourier transforming along the u or v direction is equivalent to taking the spectrally dispersed 1D fringe pattern for each orthogonal baseline orientation, and Fourier transforming with respect to frequency k . This is the same procedure that is often used for single source phase and group delay estimation (Lawson 2000, Chapter 8). Let $F(k)$ equal the product of source spectrum, throughput, and detector response. Note that since CCD's count numbers of photons, not power, F has units of numbers. The interferometer response at frequency k to a source offset from the phase center by an angle θ along the baseline B is $\frac{F(k)}{2}(1 + \cos kd) = \frac{F(k)}{2}(1 + \cos kB\theta)$ where d is the physical delay. Fourier transforming with respect to k gives $[2\tilde{F}(l) + \tilde{F}(l - d) + \tilde{F}(l + d)]/4$, with l the Fourier conjugate to k and $\tilde{F}(l)$ the Fourier transform of $F(k)$. In most cases, $F(k)$ is slowly varying, and so its Fourier transform has power mainly at low frequencies. For example, for $F(k) = \text{const}$, $\tilde{F}(l) = \delta(l)$ and the Fourier transform of the fringe pattern becomes $[2\delta(l) + \delta(l - d) + \delta(l + d)]/4$. Likewise, for a rectangular bandpass, we would have a sinc function. For simplicity, we will focus on rectangular $F(k)$, although the generalization is clear.

As expected, each source in the field of view appears as a narrow peak in the Fourier transform space (actually a pair since the brightness is a real quantity). Also note that half of the power lies at zero frequency, due to the $1/2$ which offsets the average fringe intensity from zero. Figure 2 illustrates the pattern for two point sources.

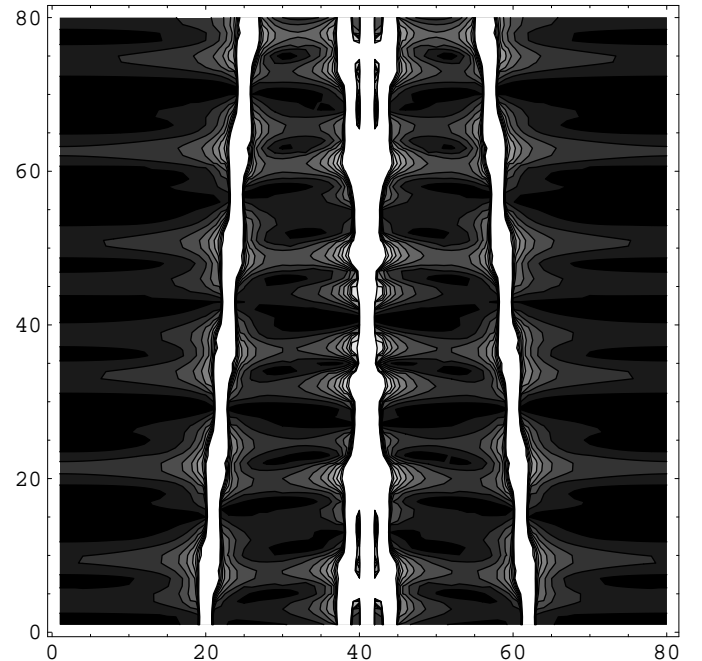


FIG. 2.— Fourier transform of the channeled spectrum with two equally bright sources, one at the phase center and the other at 250 mas. The abscissa is the Fourier conjugate to wavenumber, the ordinate is delay, and the numbers along the axes label pixels. Note that sources appear as lines in the Fourier transform, which cross at the position (delay) of the respective source. Additional sources should appear as additional, distinct lines. This figure neglects photon noise, which can hide the signal from faint sources.

Now, assume that SIM uses n_c frequency channels. For simplicity, we take each channel to have the same frequency width. This assumption allows the use of the FFT, otherwise a more general discrete Fourier transform or Lomb-Scargle periodogram would be used. With this assumption, the Nyquist theorem tells us that each bin in Fourier space has a size equaling the white-light coherence envelope size $\lambda_{\max}\lambda_{\min}/[B(\lambda_{\max} - \lambda_{\min})]$ which for a rectangular $0.4 - 1.0 \mu\text{m}$ bandpass and 10 meter baseline is roughly 13.75 mas. This makes sense, since SIM should be able to resolve sources separated by more than one coherence envelope size. Clearly, decreasing the effective bandwidth should diminish SIM's ability to resolve point sources. Varying the number of channels should affect only aliasing. With fewer, broader channels, a source near the edge of the field of view has reduced fringe contrast and would be mistaken for the combination of a fainter source near the middle of the FOV and uniform surface brightness. This could corrupt astrometric measurements of sources towards the edge of the field of view.

We have simulated SIM astrometric measurements of crowded fields with the above considerations. We assume that SIM scans repeatedly over a small range in delay, corresponding to the central fringe size at the mean frequency, which for a 10 m baseline and $0.4 - 1.0 \mu\text{m}$ bandpass is 11.8 mas. We divide this range into n_d bins 1 mas large, and integrate the fringe pattern $f(k, d) = F_i(1 + \cos kd)/2$ over $n_d \times n_c$ total bins, where $n_c = 64$ is the number of wavelength channels spanning the bandpass. We sum the contributions for all sources in the field of view, and approximate photon noise by adding to each bin a random number of photons drawn from a Gaussian with $\sigma = \sqrt{N}$. We neglect all instrumental noise, such as read noise, dark current, thermal drift, etc., basically assuming that SIM is a perfect astrometer. These additional errors may become important for the faintest sources. To simulate SIM astrometry and photometry, we fit the resulting fringe pattern to the form

$$N_{\text{model}} = N_0 + \sum_i N_i \frac{1 + \cos kB(\theta - \theta_i)}{2}.$$

The number of sources, their positions and brightnesses are first estimated using the Fourier transform method described above. Starting with these initial values we fit by minimizing the error function $\chi^2 = \sum_{i,j} (N_{ij,\text{data}} - N_{ij,\text{model}})^2 / N_{ij,\text{data}}$. The fitted parameters are each source's brightness N_i and position θ_i , as well as uniform surface brightness N_0 . This assumes that the product of the source spectrum, throughput, and detector response is constant with respect to wavelength, but it is not difficult to generalize to include simple spectral dependence.

An estimate of the centroiding precision possible by such fringe fitting may be computed using the minimum variance bound, hereafter MVB (Gould 1995). When fitting data to a function $f(x)$ with normalization and one additional parameter x_0 , the minimum variance expected in the fitted x_0 is

$$\text{var}(x_0) \equiv \sigma_{x_0}^2 = \frac{1}{N} \left[\left\langle \left(\frac{d \ln f}{dx_0} \right)^2 \right\rangle - \left\langle \frac{d \ln f}{dx_0} \right\rangle^2 \right]^{-1}$$

where $\langle g \rangle \equiv (\int f g dx) / (\int f dx)$. Using the MVB formula, and taking N total photons from a single point source, we

expect centroiding errors $\sigma_\theta = 1.87N^{-1/2}$ mas for scans covering 11 mas and the wavelength range $0.4 - 1 \mu\text{m}$. Using the white-light fringe pattern ($n_c=1$) we expect $\sigma_\theta = 2.91N^{-1/2}$ mas. So for $N = 340,000$ photons we expect 3.2 μas and 5 μas errors for the spectrally dispersed and white-light fringe pattern, respectively. This analytic estimate compares well with a Monte Carlo calculation of the expected astrometric errors using the above fringe fitting procedure. Using bins of size 1 mas ($n_d \approx 11$) gives errors of 3.8 μas and 5 μas , in agreement with the MVB estimate for white-light fringes and somewhat larger than the MVB estimate for the spectrally dispersed fringe pattern. Increasing the number of bins to ~ 100 gives Monte Carlo estimates in agreement with the MVB estimate. One might conclude from this that it is always better to centroid using spectrally dispersed fringes rather than broadband, white-light fringes since the errors are smaller for a given number of photons. However, keep in mind that we have neglected additional errors such as read noise, and there may be a reduction in throughput when the fringes are spectrally dispersed.

3. FITTING MULTIPLE SOURCES

Having confirmed that our Monte Carlo errors agree with analytic estimates for single sources, we now explore errors for multiple sources. As mentioned earlier, additional sources in the field of view can increase astrometry errors by contributing extra photon noise, and by distorting the fringe shape. Fitting for multiple sources cannot remove photon noise, but it can mitigate the distortion arising from superimposed fringes. To ease the comparison with unblended centroiding as described in the previous section, we set the on-source integration time to equal the time necessary to accumulate 340,000 photons from the science target. In terms of a signal-to-noise ratio (S/N), this holds fixed the signal while letting the noise vary. When gauging how well fitting can remove the effects of blending, we should compare to a case with the same ratio of signal (photons from science target) to noise (square root of total number of photons). For example, consider centroiding a single star in the presence of uniform surface brightness that contributes an equal number of photons as the star. Since the S/N is smaller by a factor of $\sqrt{2}$ relative to the isolated star case, the centroiding errors will be greater by a factor of $\sqrt{2}$.

As our first example, we consider measurements of a bright microlensing event in the LMC. We place a $V = 19$ target at the phase center, and randomly place field stars in the 800 mas FOV. The number of field stars, and their luminosity function (LF), are chosen to match the crowding and LF of the LMC derived by the MACHO project (Alcock et al. 2001). On average, MACHO finds 10-16 field stars within 1-2" of each observed star. To be conservative, we have used 16 field stars in all of our simulations. The average brightness of a star drawn from this LF is approximately 1.4% the brightness of a $V = 19$ star, so by adding 16 of them, we add approximately 22% more photons. We thus expect a roughly 10% increase in astrometry errors from photon noise alone. Since we normalize the on-source observation time to give us 3.8 μas photon noise errors from the $V = 19$ source alone, we expect 4.2 μas errors from photon noise. Any additional errors will

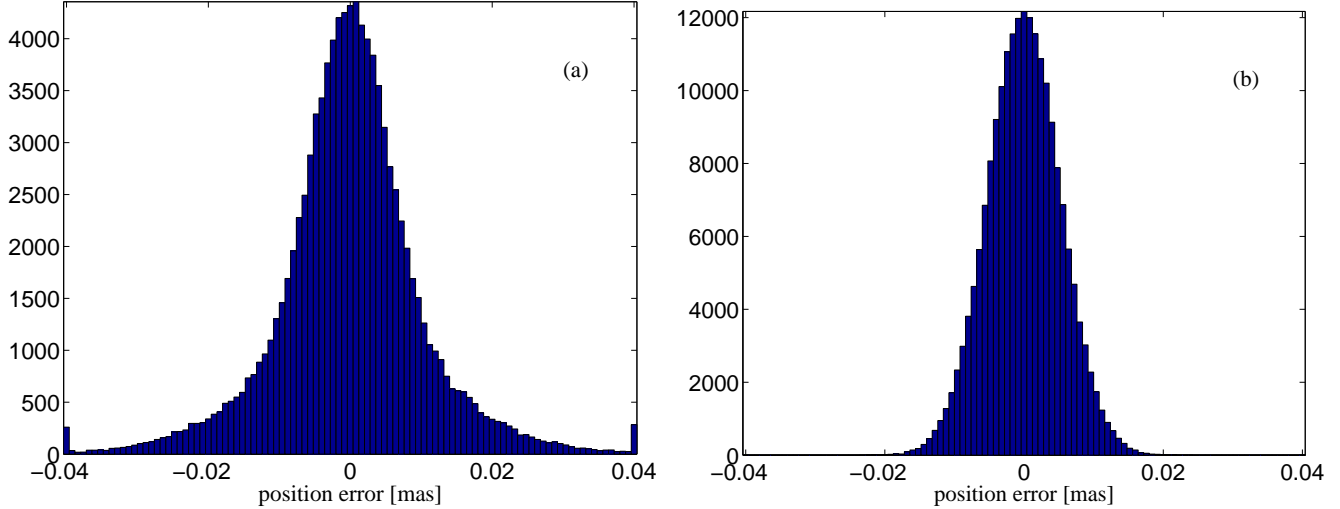


FIG. 3.— Histogram showing position residuals for multiple source fitting to $V = 19$ source and 16 stars drawn from LMC luminosity function. The first panel shows the histogram for random placement of stars. The peaks at the edge of the plot are due to events falling outside the histogram range. The second panel shows the histogram for the same calculation, restricting sources to lie more than 25 mas from the target at the phase center. See the text for more details.

be due to source confusion (Rajagopal et al. 2001).

We follow the same fitting procedure described above, allowing for multiple sources at different positions and with different brightnesses. Note, however, that faint sources may not be detectable above photon noise, so we will only be able to remove the brightest sources. Since in this example we are only interested in the measurement errors for our single target, we only report measurement errors for the $V = 19$ target. Panel (a) of Figure 3 shows the histogram of position residuals for this simulation. Overall, the standard deviation of this error distribution is $\sigma_\theta = 10.5 \mu\text{as}$, much larger than the $4.2 \mu\text{as}$ errors expected from photon noise. Note, however, that the histogram may not be well described by a single “average” error value. We find that the error distribution is characterized by a narrow core superimposed on a slowly decaying tail of outliers. This histogram is quite similar to that found by Rajagopal et al. (2001), although for different reasons. In their simulations of white-light astrometry in crowded fields in M31, the LMC and Galactic Bulge, the long tail was due to the occasional bright field star. Here, in contrast, bright field stars are easily identified and removed using dispersed fringes. The long tail here is due to the occasional star landing nearby our target and becoming unresolved from it. To demonstrate this point, panel (b) of Figure 3 shows the histogram for the same simulation, but here we restrict field stars to lie more than 25 mas from our target. Note that the long tails have vanished, and that the distribution’s standard deviation has significantly diminished, to $5.3 \mu\text{as}$, near to the value expected from photon noise. Clearly, almost all of the $10.5 \mu\text{as}$ errors in this case arise from unresolved or marginally unresolved stars falling close to the target. Rajagopal et al. (2001) have shown that these quite significant errors largely cancel for proper motion measurements, and so for many SIM applications they are not a worry. For microlensing, however, confusion errors will be a problem in crowded fields. This is because microlensed stars undergo different proper motions than other stars in the field (even

binary companions), and their brightnesses vary during the course of the lensing event. Therefore, the cancellation of errors that occurs for typical proper motion measurements will not occur here, and we expect proper motion errors of the same magnitude as the large position errors found above. Fortunately, as we show below, it is still possible to disentangle the blend effect using the complete set of position measurements. Thus, even in this most badly affected case, it is still possible to recover accurate masses and distances from astrometric microlensing events.

Generally, blend stars in SIM observations will be far fainter than the intended science targets, which are chosen for their brightness. However, it is still worthwhile to consider what effects comparably bright sources would have. To quantify this, we simulate SIM measurements of two equally bright stars in the field of view. Again we normalize the on-source integration time to give 340,000 photons from the science target. Photon noise alone should thus give us errors of $\sqrt{2} \cdot 3.8 \mu\text{as} = 5.4 \mu\text{as}$. We plot the results of our simulations in Figure 4. We can distinguish three kinds of blends from this figure. First, note that bright blends falling outside the central fringe are resolved by SIM and can be removed. The offsets due to such sources are consistent with zero, and the dispersions ($\approx 6 \mu\text{as}$) are not much larger than what is expected from photon noise alone. Clearly, such blends pose no threat to SIM astrometry using spectrally dispersed fringes. The average offset is not zero, however, for sources falling within the central fringe. Sources at distances ≤ 2 mas are completely unresolved by SIM. As expected, then, the measured centroid falls at the center of light, which is 0.5 mas for an equally bright blend at 1 mas, and 1 mas for an equally bright blend at 2 mas. Note that although the offset is large, the standard deviation is small. This is just what we expect; two equally bright sources at 0 and 1 mas should appear to SIM to be a source twice as bright located at 0.5 mas, and so the errors should be smaller by a factor of $2^{-1/2}$ compared to single source astrometry. The only blend positions giving significant errors are those that are

marginally unresolved, i.e. falling barely inside the central fringe, at separations of 3-4 mas. There would seem to be no way to handle such blends with a single baseline orientation, however an additional pointing along a different baseline orientation could resolve the two sources.

It is apparent from Figure 4 that the vast majority of bright field stars will pose no threat to SIM astrometry. The fact that the fit residuals are so small, comparable to photon noise, means that fitting can reliably remove the fringes from blending sources in the field of view. Since we are able to recover μ as astrometry even in the presence of blends, this must mean that we are able to fit the blend positions to microarcseconds themselves. Since we are doing this for all important blends in the field of view, we are basically imaging the field of view. It is therefore interesting to explore the imaging capabilities of SIM using just the spectrally dispersed fringes measured along two orthogonal baselines. From the discussion above, we expect that we can get reliable positions as long as the sources are separated by more than one white-light coherence envelope. In terms of the Fourier transform space, we expect to measure reliable positions for sources separated by more than one pixel. With n_c wavelength channels, we have $n_c/2$ distinct pixels in the Fourier conjugate variable since the brightness is real. We have assumed 64 channels, so we have 32 pixels. Assuming that sources should be separated by 3 pixels for reliable positions means that we expect that for up to 10 sources in the FOV, we can measure positions reliably. To test this, we simulated SIM astrometric measurements of 10 stars in the field of view. We first simulated 10 stars of equal brightness; the results are shown in panel (a) of Figure 5. We find that the astrometric errors scale like $t^{-1/2}$ where t is the on-source integration time, so they are mainly due to photon noise.

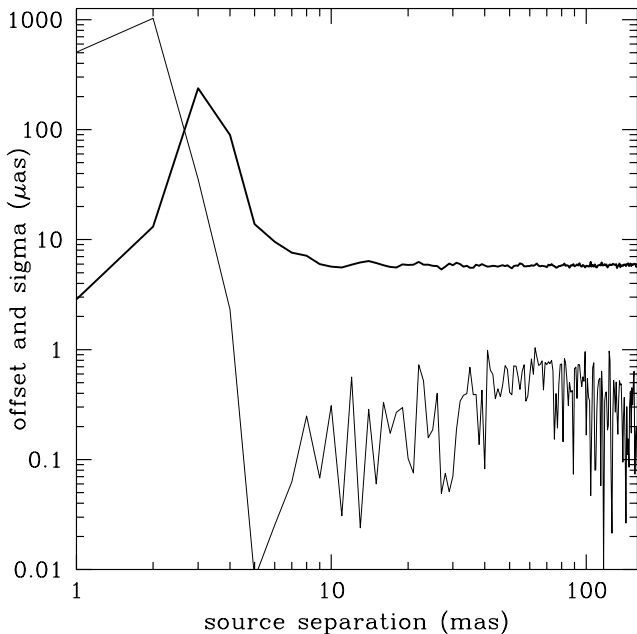


FIG. 4.— Fit residuals for astrometric measurements of a single star, with an equally bright blend in the field of view, as a function of distance to the blend. The thin curve is the average offset of the fit source position from the input position and the thick curve is the standard deviation of those offsets.

For the simulation plotted in panel (a), the astrometric errors were $\sigma = 6 \mu$ as. In panel (b), we plot the scaling of errors with brightness. Using the above arguments on S/N, we expect the errors to scale inversely with each star's brightness, and this is verified in Figure 5(b). Clearly, far smaller errors are attainable using dispersed fringes than the $\sim 250 \mu$ as errors expected from synthesis imaging of many baseline orientations (although keep in mind that we have neglected errors such as thermal drift). Thus, it is possible that highly precise astrometric imaging may be achieved using only two SIM pointings.

4. APPLICATION: ASTROMETRIC MICROLENSING

One possible application of SIM astrometry in crowded fields is microlensing. There are numerous astrophysical applications of SIM observations of microlensing events (Paczynski 1998; Boden et al. 1998; Safizadeh et al. 1999; Gould & Salim 1999; Salim & Gould 2000), most of which entail crowded fields. For ordinary proper motion, Rajagopal et al. (2001) have shown that astrometric errors arising from source confusion largely cancel. This is because any offset caused by additional sources remains basically constant as the target executes its proper motion, and cancels when the relative motion of the target is measured. However, this is not true for microlensing. The reason for this is that microlensing changes the target's apparent brightness while also causing the apparent proper motion. The astrometric offset caused by blending, therefore, does not remain constant and will not cancel. Thus, we might expect that blending could seriously damage microlensing measurements, rendering SIM observations useless in crowded fields. Fortunately, the results discussed in previous sections indicate that blending by bright stars should not corrupt SIM astrometry, except when those sources fall within the white-light coherence envelope of the target star. However, binary companions to lensed stars could easily fall inside the central fringe. Since fringe fitting could never detect such stars, just as fringe fitting cannot resolve the two microlensed images, our concerns about crowding could still hold. Fortunately, as we describe below, even sources falling within the central fringe may be detected and removed, not from individual SIM measurements, but by using the entire set of observations of the microlensing event.

As discussed in the previous section, field sources may be detected and essentially removed as long as they lie outside the central fringe of the target. In fact, even marginally resolved sources falling barely within the central fringe may be detected and removed if bright enough, by the distortion they cause in the fringe shape. The only sources undetectable are those which do not distort the fringe shape, but merely shift its centroid. These sources, lying well inside the central fringe, shift the fringe centroid to the center of light of the target and blend, and add all of their light to the target. What SIM would detect would be a star of brightness equaling the sum of the target and blend's brightness, located at their center of light. For this reason, multiple blends falling inside the central fringe are equivalent to a single blend, and so we consider only the single blend case. Such blends affect the microlensing lightcurve and astrometric motion in a simple way (Han & Kim 1999), and we show that SIM observa-

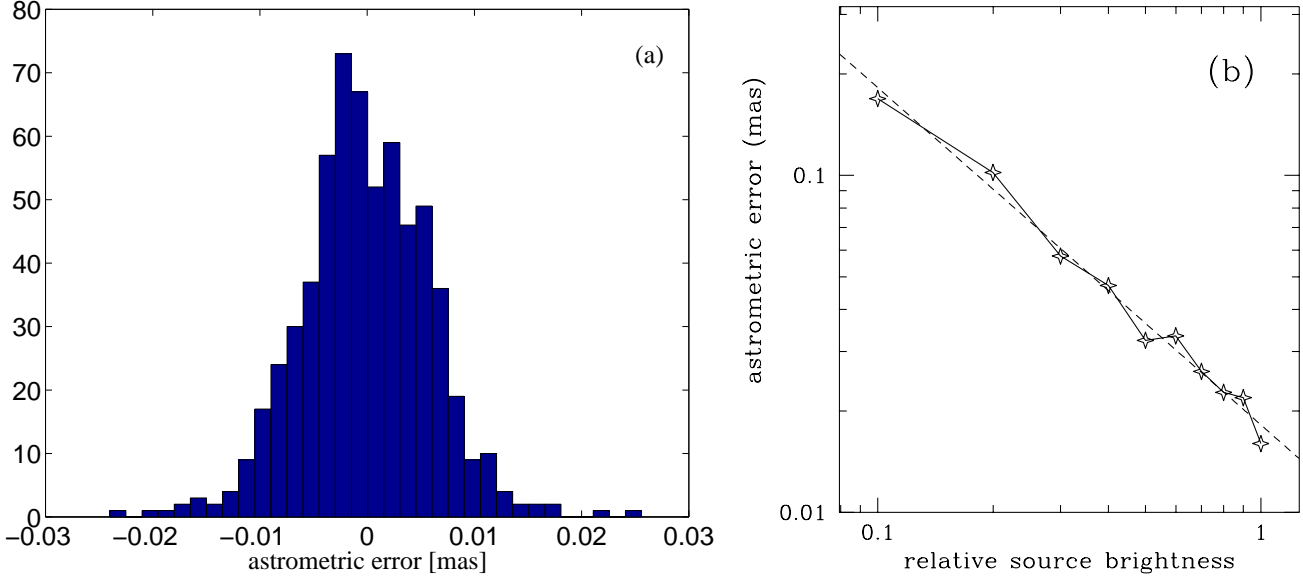


FIG. 5.— Simulated astrometric imaging errors for 10 sources. Panel (a) show the error histogram from a simulation of imaging of 10 equally bright sources in the 800 mas field of view. The standard deviation of this histogram is $\sigma = 6 \mu\text{as}$. Panel (b) shows the scaling of error with brightness for a simulation of 10 sources with varying brightnesses. Plotted points are errors as a function of brightness relative to the brightest star in the field. The dashed line is not a fit, but shows the expected scaling: error inversely proportional to brightness.

tions may be corrected without degeneracy to extract the desired measurables.

It is first necessary to review astrometric microlensing; see Boden et al. (1998) for more details. Microlensing of a single source by a single lens gives two images of the source. If the source is located at position $\vec{x}_s = \theta_E \vec{u}$ relative to the lens, then the two images appear at positions with magnifications

$$\vec{x}_{1,2} = \theta_E(u \pm \sqrt{u^2 + 4})/2$$

$$A_{1,2} = \frac{u^2 + 2}{2u\sqrt{u^2 + 4}} \pm \frac{1}{2}.$$

Here, θ_E is the angular Einstein radius, $u = |\vec{u}|$ is the lens-source separation in units of θ_E (not the u from the u, v plane), and positions are relative to the lens position. SIM cannot resolve these images, so in the absence of blending it detects a source with position $\vec{x} = \vec{x}_s + \vec{\Delta}x$ and magnification A given by

$$\vec{\Delta}x = \theta_E \frac{\vec{u}}{u^2 + 2}, \quad A = \frac{u^2 + 2}{u\sqrt{u^2 + 4}}.$$

Note that $\vec{\Delta}x$ traces out an ellipse.

It is now easy to see how unresolved blends affect this. If the lensed source has unlensed brightness F_s , and the blend has brightness F_b and position \vec{x}_b , then SIM detects a source at position \vec{x}_{obs} with brightness F_{tot} given by

$$F_{\text{tot}} = AF_s + F_b, \quad \vec{x}_{\text{obs}} = \frac{AF_s(\vec{x}_s + \vec{\Delta}x) + F_b\vec{x}_b}{F_{\text{tot}}}$$

An example of this is given in Figure 6. From the illustration, it may appear that blending would ruin SIM astrometry, since the observed motion bears little resemblance to the unblended motion. However, our simulations indicate that it will be possible to recover the unblended motion. This is largely because SIM's exquisite photometry (recall $N \gtrsim 340,000$) permits the nondegenerate decomposition

of the photometric lightcurve into lensed and unlensed (blend) light. That is, F_s , F_b , and A may be measured from the photometry alone. Given the blend fraction, we now show that it is easy to fit the astrometric data to recover the microlensing parameters θ_E , $t_E \equiv |\vec{u}|^{-1}$, etc., which are then used to determine the lens mass and distance.

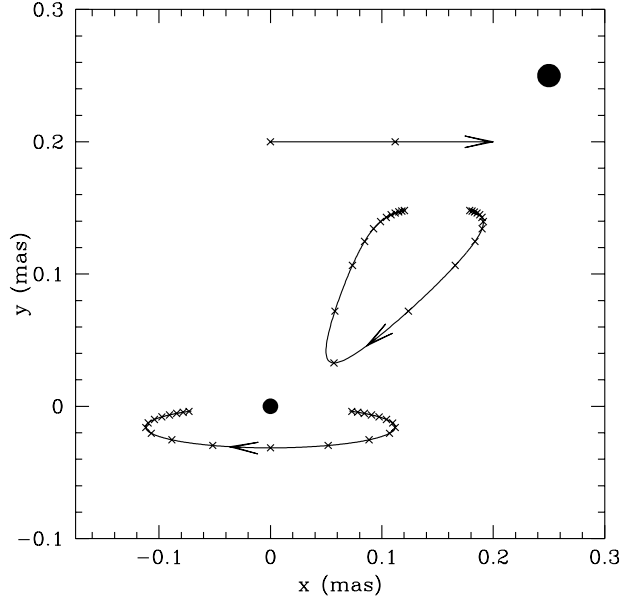


FIG. 6.— Microlensing source and motion of lens and image center-of-light. The large dot shows the location of the blend star, the small dot the location of the target star. The straight arrow shows the location and relative motion of the lens near the peak of the event, with x's placed every week. $t_E = 20$ days and $\theta_E = 0.32$ mas. The elliptical curve asymptotic to the target source shows the unblended astrometric motion of the image center of light, while the irregular curve is the observed motion of the center of light including the blend star light. Arrows show the direction of motion.

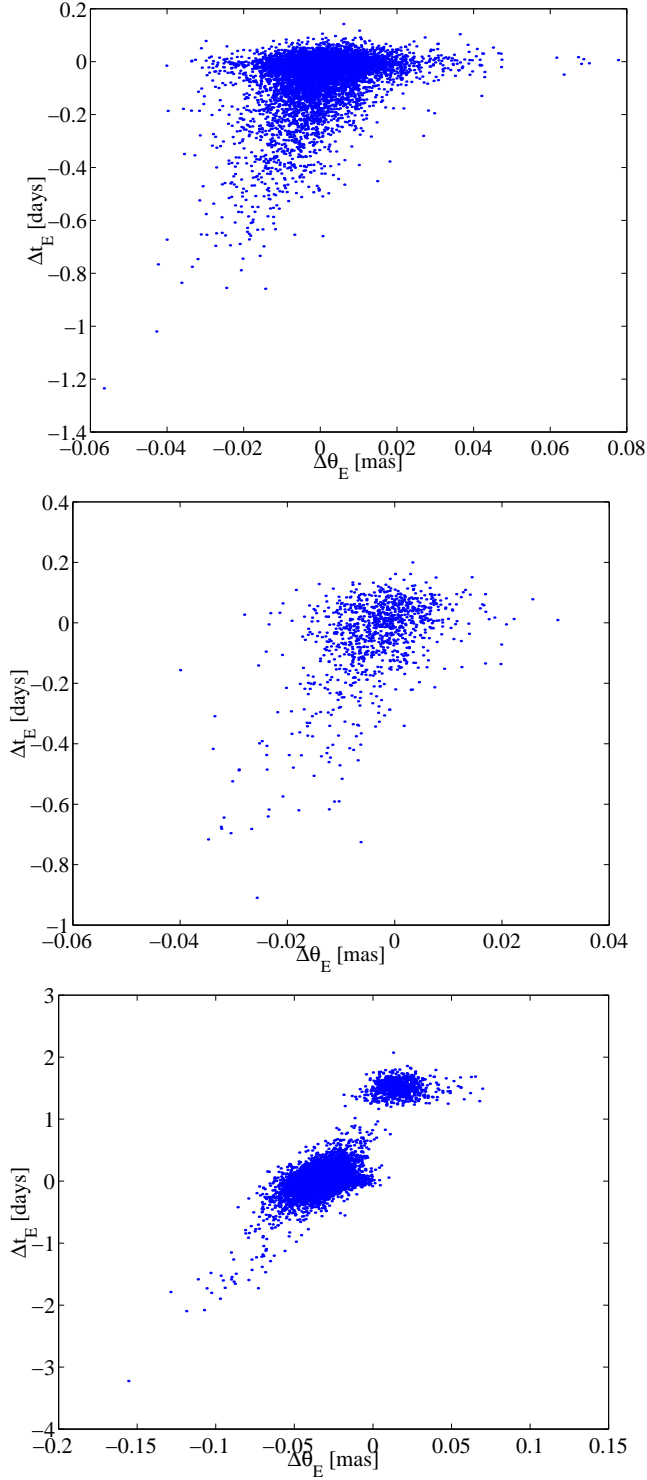


FIG. 7.— Fit residuals for microlensing event. Each point in the scatter plot represents a different simulated event; plotted are the residuals in fitted θ_E and t_E . 10,000 simulations of unblended microlensing events are plotted in the first panel; the standard deviations are $\sigma_\theta = 0.009$ mas and $\sigma_t = 0.1$ days, for input values $\theta_E = 0.32$ mas and $t_E = 20$ days. In the second panel, we plot 1000 simulations of microlensing events with a $V = 19$ target near the phase center and 16 additional stars drawn from LMC luminosity function placed randomly in FOV. Here, the standard deviations are $\sigma_\theta = 0.008$ mas and $\sigma_t = 0.14$ days for the same input parameters as the unblended case. The last panel plots errors for 10,000 simulations of microlensing events with 16 field stars, but with white-light fringe fitting. Here, θ_E is systematically underestimated by 0.03 mas (roughly 10%), with a dispersion of 0.017 mas, while t_E has a dispersion of 0.44 days.

The blended microlensing event is parametrized by 11 quantities: the above mentioned θ_E , t_E , \vec{x}_s , \vec{x}_b , F_s , and F_b , as well as the normalized impact parameter u_{\min} , time of closest approach t_0 , and relative proper motion direction ϕ . For simplicity we assume that the same blend brightness F_b applies for both the x and y astrometric measurements. This will not be true in general (a field star whose projected position relative to the target happens to fall inside the central fringe under one orientation need not fall inside the central fringe along the orthogonal orientation). However, it is trivial to generalize our treatment to include two different blends for the x and y measurements. We have also assumed that the blend's proper motion is negligible for simplicity, but again it should not be difficult to generalize to moving blends. Now, the photometry alone gives us t_0 , t_E , u_{\min} , F_s , and F_b . The remaining 6 parameters are to be derived from the astrometry. First note that the unblended astrometric motion along the relative proper motion vector is antisymmetric in time with respect to t_0 , while the unblended motion perpendicular to it is symmetric (see Figure 6). The blend position and brightness are constant, and therefore symmetric. So if we multiply \vec{x}_{obs} by F_{tot} , and antisymmetrize in time with respect to t_0 , then the blend parameters drop out, and the resulting motion is along the unblended proper motion vector. So we immediately get ϕ . We can estimate θ_E from t_E , u_{\min} and the velocity \vec{x} at peak. Again, note that the blend parameters make a constant contribution to the product $F_{\text{tot}}\vec{x}_{\text{obs}}$, so by taking the difference of this quantity evaluated at two different times, the blend parameters drop out. We can thus estimate the unlensed source position \vec{x}_s by using the estimates for the other parameters, and the change in $F_{\text{tot}}\vec{x}_{\text{obs}}$ from peak to the end of the event. Now we have estimates for all parameters except the blend position \vec{x}_b , which we can guess by comparing the measured $F_{\text{tot}}\vec{x}_{\text{obs}}$ with the contributions from the other terms. Thus, we can simply and accurately guess values for all of the microlensing parameters, and use these as initial estimates for fitting routines. This is also true if there are different blend fractions for the two baseline orientations.

To quantify the above statements, we have simulated SIM observations of microlensing events. Each of our simulated events has $\theta_E = 0.32$ mas and $t_E = 20$ days. The other parameters, such as u_{\min} , ϕ and \vec{x}_s were picked randomly. We measure 25 points during the event, evenly spaced in time, starting when the apparent magnification exceeds a threshold $A > A_{\text{th}} = 1.5$, and lasting $5t_E$ from the trigger. This is probably not an optimal observing strategy, but it is not our intention here to optimize the strategy. Each astrometric measurement is made following the procedure described in previous sections – the fringe pattern is simulated and fitted to recover the source position and brightness. We assume that the x and y measurements occur at the same time, although this assumption has no effect. If SIM measures the orthogonal baselines at different times, say to minimize its overall slewing, no information should be lost. Even if the baselines are not perfectly orthogonal, measurements of the microlensing parameters should not be seriously degraded.

To measure how badly crowding affects microlensing measurements, we first see how well the parameters may be

recovered for a single, unblended source. To save on computation time, we used white-light fringe measurements, which as noted above should not be much worse than spectrally dispersed measurements for unblended sources. Now, to measure the lens mass and distance, the parameters of interest are θ_E , t_E , and ϕ . In the first panel of Figure 7 we plot fit residuals for the above observing strategy. Note that these fits utilize both SIM astrometric and photometric measurements of the microlensing events. We find that θ_E can be measured to 2.84%, and t_E to 0.5%, for input values of $\theta_E = 0.32$ mas and $t_E = 20$ days.

Now, we add blend stars to see how badly they affect microlensing mass and distance measurements. Here, we clearly need to use the full multifrequency fringe fit to resolve bright blend stars. From the individual fringe fits, which gave errors $\sim 10 \mu\text{as}$ (twice as large as the unblended errors) we might think that the errors here would be twice as large. We plot the fit residuals in the second panel of Figure 7. We obtain errors $\sigma_\theta = 0.008$ mas, $\sigma_\phi = 0.0235$, and $\sigma_t = 0.142$ days. Normalized to $\theta_E = 0.32$ mas and $t_E = 20$ days, these are fractional errors of 2.5%, 2.4%, and 0.71% respectively, as good as or better than the unblended white light errors! Again, the reason that these errors are not twice as big as the unblended errors is that the relatively large single measurement residuals mainly arose from unresolved sources falling inside the target's central fringe, which as we discussed may easily be removed.

Another important question to ask is how badly we would do without the spectral decomposition of the fringe pattern. To address this question, we repeated the above simulations, but this time used only white-light fringes. The resulting errors are plotted in Figure 7. We find that the error distribution is bimodal, and neither blob is centered on the correct answer! The bulk of the fits underestimate θ_E by roughly 10%, with a scatter of $\sim \pm 5\%$, although a subset of events give somewhat overestimated θ_E , about 5% too large, with a scatter of $\sim \pm 3\%$. This "more correct" subset, however, overestimates t_E by roughly 8%. So if we were to fit a white light measurement of a microlensing event in the LMC, we could be reasonably certain that the derived masses and distances would be incorrect by about 20%. While 20% distances would certainly be good enough to resolve the question of the location of the LMC lenses, it is clearly preferable to utilize the channeled spectrum when possible.

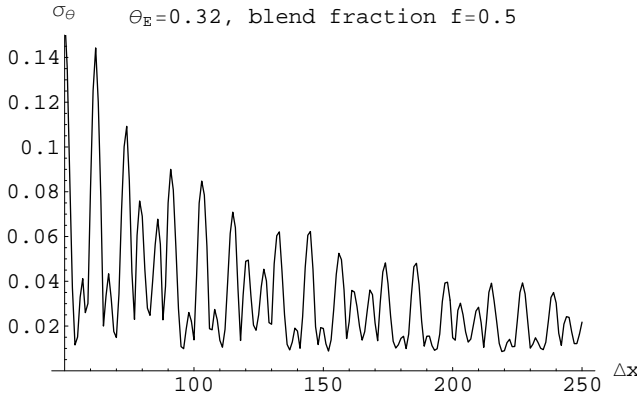


FIG. 8.— Fit residuals for microlensing event with an equally bright blend in FOV, fitting to the white-light fringe pattern. We only plot for distances large compared to the fringe size; closer separations give much larger errors. σ_θ is in mas.

We should be careful, however. Most field blends drawn from the LMC luminosity function are less than a few percent of the brightness of a $V = 19$ star. A comparably bright star landing in the field of view could corrupt measurements based upon white-light fringes (Rajagopal et al. 2001). To illustrate this, we simulate white light SIM measurements of microlensing events with an equally bright source in the field of view. Now, it should be clear that sources within a few fringes of the target will hopelessly corrupt our measurements. However, sources falling outside the coherence envelope have significantly diminished fringe contrast, and one might hope that their effect would be minimal. These hopes are unfounded, as figure 8 illustrates. This figure plots the errors in θ_E as a function of source separation (both in mas). Even sources lying more than 100 mas away can induce 20% errors in the fit. A caveat to this statement is that the assumption of rectangular bandpass overestimates the effect of distant sources. The discontinuous jumps in $F(k)$ at the edges of the bandpass give sidelobes in the white-light fringe envelope, which would be suppressed with a more smooth decline. Nevertheless, distant bright sources are clearly cause for concern when centroiding white light fringes. Now, space telescope or ground based AO snapshots could detect such sources. However, the positions available from such snapshots are rough by SIM standards, $\sim 20 - 40$ mas, which is larger than a fringe size and larger than the length scale of the variations exhibited in Figure 8. Thus, such high resolution snapshots would not be helpful for fitting multiple sources.

How much better do we do if we have dispersed fringes? As previous sections showed, bright sources landing outside the central fringe are easily detected and removed. Therefore, such sources will not corrupt SIM microlensing events beyond adding photon noise, which can be alleviated by integrating longer. We might worry about closer sources, however. Figure 9 shows results from the same simulation as above, but for blends within 50 mas, using the channeled spectrum. The errors are all small ($\sim 3\%$) except for marginally resolved blends at about 3 mas separation which have 10-20% errors. Bright sources at this distance fall within the central fringe and cannot be clearly resolved, but are not well enough inside the central fringe to be treated as completely unresolved. In contrast, faint sources at this distance are effectively unresolved.

This shows the extent to which spectrally dispersed fringes are useful. If the spectral decomposition of the fringe pattern is unavailable or costly to transmit, and we must rely upon white-light fringes, then high resolution space telescope or AO images will be required before following up a microlensing event with SIM. Detection of a bright field source in such snapshots would not help us remove the blend's effect, but instead would tell us that such events are hopelessly corrupted and should not be followed by SIM. Since bright events in the LMC are rare, and snapshots would tell us nothing about possible blends $\lesssim 40$ mas from the target which would also corrupt SIM measurements, we hope that spectrally dispersed fringes will be available in the final SIM design. High resolution snapshots may be useful with dispersed fringes as well, since they could be used to avoid orientations that project bright field stars inside the target's central fringe.

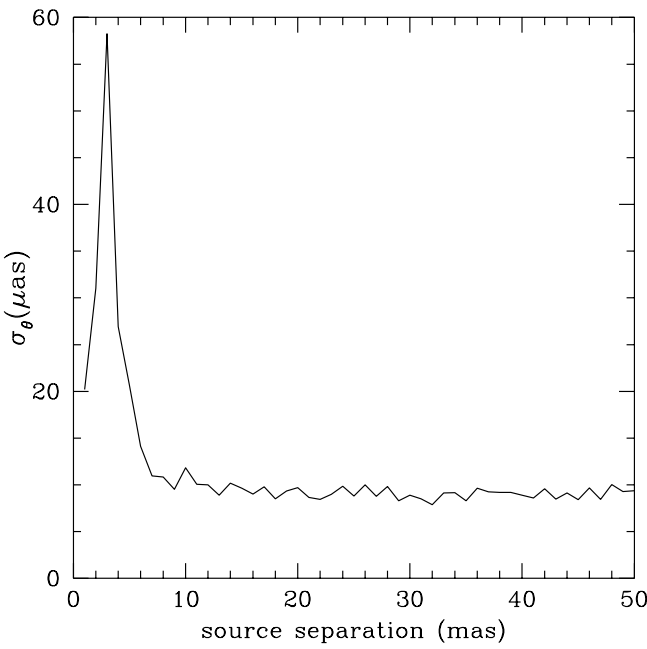


FIG. 9.— Fit residuals for microlensing event with equally bright blend star and 15 other blends drawn from LMC luminosity function. The 15 faint LMC blends are placed randomly in field of view, and errors are plotted as a function of the bright blend position. Compare this curve with Figure 4.

5. SUMMARY

We have shown that the spectral decomposition of the fringe pattern, which is often used for group delay estimation, also allows highly precise astrometry to be performed in crowded fields. Even when white-light fringes are hopelessly corrupted, dispersed fringes allow microarcsecond positions to be measured. We find that any significant source outside of the central fringe (> 6 mas) of the target star may be detected and removed by fitting the two di-

mensional (delay *vs.* wavelength) fringe pattern, thereby restoring SIM astrometry to the precision (few μ as) expected for isolated sources. We have further shown that in mildly crowded stellar fields, precise astrometric imaging is possible using fringes in the channeled spectrum, with positional precision comparable to that expected for single star astrometry. Although the details will depend upon SIM’s precise characteristics, we expect that imaging should be possible for up to 10 comparably bright sources in the field of view.

We then illustrated our method with the specific example of astrometric microlensing. We showed that, although unresolved sources falling within the central fringe could corrupt individual astrometric measurements, accurate masses may still be measured by fitting the entire microlensing event. In this manner, confusion or blending errors may be brought below photon noise errors. For the worst case, i.e. LMC events which are the most crowded and have relatively faint sources, 5% mass measurements are still easily attainable. We also considered the effect of exceptionally bright field stars or binary companions, and showed that for all separations except about 3 mas, such bright sources also do not adversely affect SIM astrometry. Chance separations of 3 mas, however, can lead to 20% errors in mass and distance measurements from microlensing events.

In conclusion, we find that SIM astrometry will not be corrupted by blending, and extremely precise imaging of mildly crowded fields may be performed using only two orthogonal baseline orientations, allowing microarcsecond positional measurements.

We thank Andy Boden, Andy Gould, and Andreas Quirrenbach for many helpful discussions and suggestions, and Jayadev Rajagopal for helpful discussions, suggestions and for sending us an advance copy of his paper. This work was supported in part by the U.S. Dept. of Energy under grant DEFG0390ER40546. ND was also supported in part by the ARCS Foundation.

REFERENCES

Alcock, C. et al. (MACHO collaboration) 2001, ApJS submitted, preprint astro-ph/003392.
 Allen, R. et al. 2000, “Crowded-Field Astrometry and Imaging with the Space Interferometry Mission”, http://sim.jpl.nasa.gov/ao_support/allen.pdf.
 Boden, A. F., Shao, M. & van Buren, D. 1998, ApJ, 502, 538.
 Dyck, H. M., Benson, J. A., & Schloerb, F. P. 1995, AJ, 110, 1433.
 Gould, A. 1995, ApJ, 440, 510.
 Gould, A. & Salim, S. 1999, ApJ, 524, 794.
 Han, C. & Kim, T. 1999, MNRAS, 305, 795.
 Koechlin, L., Bonneau, D., & Vakili, F. 1979, A&A, 80, L13.
 Lawson, P. R. 2000, *Principles of Long Baseline Interferometry*, <http://sim.jpl.nasa.gov/library/coursesnotes.html>.
 Paczyński, B. 1998, ApJ, 494, L23.
 Quirrenbach, A. 1997, “Interferometry in Practice”, in *Science with the VLT Interferometer, Proceedings of the ESO workshop, held at Garching, Germany, 18-21 June 1996*, Springer-Verlag: Berlin.
 Rajagopal, J., Böker, T., & Allen, R. 2001, “The confusion limit on astrometry with SIM”, preprint to be submitted to ApJ.
 Safizadeh, N., Dalal, N., & Griest, K. 1999, ApJ, 522, 512.
 Salim, S. & Gould, A. 2000, ApJ, 539, 241.
 Schloerb, F. P. 1990, in Breckinridge, J. B., ed., *Amplitude and Intensity Spatial Interferometry*, Proc. SPIE, 1237, 154.
 Thompson, A. R., Moran, J. M., & Swenson, G. W. 1986, *Interferometry and Synthesis in Radio Astronomy*. Wiley: New York.